

# Pair distribution function of the spin-polarized electron gas: A first-principles analytic model for all densities

Paola Gori-Giorgi<sup>1</sup> and John P. Perdew<sup>2</sup>

<sup>1</sup>*INFM Center for Statistical Mechanics and Complexity and Dipartimento di Fisica,  
Università di Roma “La Sapienza”, Piazzale A. Moro 2, 00185 Rome, Italy*

<sup>2</sup>*Department of Physics and Quantum Theory Group,  
Tulane University, New Orleans, Louisiana 70118 USA*

(Dated: May 21, 2019)

We construct analytic formulas that represent the coupling-constant-averaged pair distribution function  $\bar{g}_{xc}(r_s, \zeta, k_F u)$  of a uniform electron gas with density parameter  $r_s = (9\pi/4)^{1/3}/k_F$  and relative spin polarization  $\zeta$  over the whole range  $0 < r_s < \infty$  and  $-1 < \zeta < 1$ , with energetically-unimportant long range ( $u \rightarrow \infty$ ) oscillations averaged out. The pair distribution function  $g_{xc}$  at the physical coupling constant is then given by differentiation with respect to  $r_s$ . Our formulas are constructed using *only* known theoretical constraints plus the correlation energy  $\epsilon_c(r_s, \zeta)$ , and accurately reproduce the  $g_{xc}$  of the Quantum Monte Carlo method and of the fluctuation-dissipation theorem with the Richardson-Ashcroft dynamical local-field factor. Our  $g_{xc}$  seems to be correct even in the high-density ( $r_s \rightarrow 0$ ) and low-density ( $r_s \rightarrow \infty$ ) limits. When the spin resolution of  $\epsilon_c$  into  $\uparrow\uparrow$ ,  $\downarrow\downarrow$ , and  $\uparrow\downarrow$  contributions is known, as it is in the high- and low-density limits, our formulas also yield the spin resolution of  $g_{xc}$ . We also analyze the kinetic energy of correlation into contributions from density fluctuations of various wavevectors.

## I. INTRODUCTION, DEFINITIONS, AND OUTLINE

The exchange-correlation pair-distribution function  $g_{xc}(\mathbf{r}, \mathbf{r}')$  of an  $N$ -electron system is defined as

$$g_{xc}(\mathbf{r}, \mathbf{r}') = \frac{N(N-1)}{n(\mathbf{r})n(\mathbf{r}')} \int |\Psi(\mathbf{r}, \mathbf{r}', \mathbf{r}_3 \dots \mathbf{r}_N)|^2 d\mathbf{r}_3 \dots d\mathbf{r}_N, \quad (1)$$

where  $n(\mathbf{r})$  is the electron density and  $\Psi$  is the many-body wavefunction. Its coupling-constant average  $\bar{g}_{xc}(\mathbf{r}, \mathbf{r}')$  is equal (in the Hartree units used throughout) to

$$\bar{g}_{xc}(\mathbf{r}, \mathbf{r}') = \int_0^1 d\lambda g_{xc}^\lambda(\mathbf{r}, \mathbf{r}'), \quad (2)$$

where  $g_{xc}^\lambda(\mathbf{r}, \mathbf{r}')$  is the pair-distribution function when the electron-electron interaction is  $\lambda/|\mathbf{r} - \mathbf{r}'|$  and the density is held fixed at the physical value. The coupling-constant averaged  $\bar{g}_{xc}$  plays a crucial role in density functional theory, since it can account for the kinetic energy of correlation.<sup>1</sup> In fact,  $n(\mathbf{r}') [\bar{g}_{xc}(\mathbf{r}, \mathbf{r}') - 1]$  is the density at  $\mathbf{r}'$  of the exchange-correlation hole around an electron at  $\mathbf{r}$ .

In the uniform electron gas,  $n(\mathbf{r}) = n$  and  $g_{xc}(\mathbf{r}, \mathbf{r}')$  only depends on  $u = |\mathbf{r} - \mathbf{r}'|$ , and parametrically on the density parameter  $r_s = (3/4\pi n)^{1/3}$  and on the spin-polarization  $\zeta = (N_\uparrow - N_\downarrow)/N$ . The coupling-constant average is in this case<sup>2</sup> equivalent to an average over  $r_s$ :

$$\bar{g}_{xc}(r_s, \zeta, k_F u) = \frac{1}{r_s} \int_0^{r_s} g_{xc}(r'_s, \zeta, k_F u) dr'_s, \quad (3)$$

where  $k_F = (9\pi/4)^{1/3}/r_s$  is the Fermi wavevector.

Clearly then

$$g_{xc}(r_s, \zeta, k_F u) = \frac{\partial}{\partial r_s} [r_s \bar{g}_{xc}(r_s, \zeta, y)] \Big|_{y=k_F u}. \quad (4)$$

The high-density ( $r_s \rightarrow 0$ ) limit is the weak-interaction limit in which the kinetic energy dominates, and the low-density ( $r_s \rightarrow \infty$ ) limit is the strong-interaction limit in which the Coulomb potential energy dominates.

The exchange-correlation pair-distribution function of the uniform electron gas and its coupling-constant average are fundamental quantities in the development of semilocal<sup>3</sup> and nonlocal<sup>4,5</sup> exchange-correlation energy density functionals. They are also relevant in density matrix functional theory<sup>6</sup> (DMFT), and for building up the system-averaged exchange-correlation hole of a many electron system of nonuniform density.<sup>7</sup>

The static structure factor  $S_{xc}(r_s, \zeta, k/k_F)$  is the Fourier transform of the pair-distribution function,

$$S_{xc}(r_s, \zeta, k/k_F) = 1 + \frac{4}{3\pi} \int_0^\infty [g_{xc}(r_s, \zeta, k_F u) - 1] \times (k_F u)^2 \frac{\sin ku}{ku} d(k_F u), \quad (5)$$

and its coupling-constant average  $\bar{S}_{xc}$  is obtained by changing  $g_{xc}$  into  $\bar{g}_{xc}$  in Eq. (5). Usually  $g_{xc}$  and consequently  $\bar{g}_{xc}$ ,  $S_{xc}$ , and  $\bar{S}_{xc}$  are divided into exchange and correlation contributions:

$$g_{xc}(r_s, \zeta, k_F u) = g_x(\zeta, k_F u) + g_c(r_s, \zeta, k_F u), \quad (6)$$

where the exchange function  $g_x$  is obtained by putting a Slater determinant of Kohn-Sham orbitals (or of Hartree-Fock orbitals) into Eq. (1). For a uniform electron gas, both Kohn-Sham and Hartree-Fock orbitals are plane waves, and  $g_x$  is a simple function of  $k_F u$ . The exchange-only pair-distribution function does not depend explicitly

on  $r_s$ , so that  $\bar{g}_x = g_x$ : the explicit dependence on  $r_s$  only appears when Coulomb repulsion is taken into account in the wavefunction. Both  $g_x$  and  $g_c$  have energetically unimportant long-range oscillations.

Available analytic models<sup>2,8</sup> of  $g_c$  and  $\bar{g}_c$  for the uniform electron gas break down at high<sup>9,10</sup> ( $r_s \lesssim 0.1$ ) and low ( $r_s > 10$ ) densities. In this paper, we present a new model for the nonoscillatory part of  $\bar{g}_c$  (and hence  $g_c$ ) which fulfills most of the known exact properties and is valid over the whole ( $0 < r_s < \infty$ ) density range and for all spin polarizations  $\zeta$ . Our model is built up by interpolating between the short-range part recently computed in Ref. 11 and the long-range nonoscillatory part which is exactly given by the random-phase approximation<sup>12</sup> (RPA). Exact small- $u$  and large- $u$  expansions are recovered up to higher orders with respect to currently available models.<sup>2,8</sup> All the parameters which appear in our interpolation scheme are fixed by exact conditions. We also build up a new nonoscillatory exchange  $g_x$  which fulfills exact short-range and long-range properties up to the same order as our  $\bar{g}_c$  does.

Our interest in having nonoscillatory  $\bar{g}_c$  and  $g_x$ , valid at all densities and with the exact short- and long-range behavior up to higher orders than currently available, stems in part from their use for building up exchange-correlation energy density functionals compatible with exact exchange, and for the study of the exchange-correlation hole of systems of nonuniform density using the exact exchange hole as an input.

The paper is organized as follows. In Sec. II, we list the known exact properties of  $g_{xc}$  and  $\bar{g}_{xc}$ , and the major limitations of the models of Refs. 2 and 8. We then present our nonoscillatory model for exchange (Sec. III) and for correlation (Sec. IV). In Sec. V, we discuss our results for exchange and correlation over the whole density range. At metallic densities, we compare our analytic model with the available Quantum Monte Carlo (QMC) data,<sup>13,14</sup> finding fair agreement (Fig. 2). We also computed  $g_c$  corresponding to the dynamic local-field factors of Richardson and Ashcroft<sup>15</sup> (RA), in order to see better how our model averages out the long-range oscillations (currently not available from QMC). In this way, we are also able to show the effect of a dynamic local-field factor on the long-range oscillations, by comparing the RA result with the RPA (corresponding to zero local-field factor) long-range  $g_c$  (Fig. 3). At high density, we find that our model is in very good agreement with exact calculations<sup>9,16</sup> (Fig. 4), and at low density it does not break down and shows the expected  $\zeta$  dependence (Fig. 1). In Sec. VI, we discuss how to extend our scheme to the spin-resolved ( $\uparrow\uparrow$ ,  $\downarrow\downarrow$  and  $\uparrow\downarrow$ ) pair-distribution functions. The wavevector analysis of the kinetic energy of correlation corresponding to our  $S_c$  and  $\bar{S}_c$  is presented in Sec. VII. Section VIII is devoted to conclusions and perspectives.

## II. EXACT PROPERTIES, AND LIMITATIONS OF PREVIOUS MODELS

We list below most of the known exact properties of  $g_{xc}$  and  $\bar{g}_{xc}$  for the 3D uniform electron gas. Equation (1) implies the positivity constraint  $g_{xc} \geq 0$  and the particle-conservation sum rule, which can be divided into exchange and correlation,

$$\int_0^\infty du 4\pi u^2 n (g_x - 1) = -1 \quad (7)$$

$$\int_0^\infty du 4\pi u^2 n g_c = \int_0^\infty du 4\pi u^2 n \bar{g}_c = 0. \quad (8)$$

With the Coulomb interaction  $1/u$ , the exchange function  $g_x$ , the correlation function  $g_c$ , and its coupling-constant averaged  $\bar{g}_c$  integrate to the exchange energy  $\epsilon_x$ , to the potential energy of correlation  $v_c$ , and to the correlation energy  $\epsilon_c$  respectively,

$$\frac{1}{2} \int_0^\infty du 4\pi u^2 \frac{1}{u} n (g_x - 1) = \epsilon_x(r_s, \zeta), \quad (9)$$

$$\frac{1}{2} \int_0^\infty du 4\pi u^2 \frac{1}{u} n g_c = v_c(r_s, \zeta) \quad (10)$$

$$\frac{1}{2} \int_0^\infty du 4\pi u^2 \frac{1}{u} n \bar{g}_c = \epsilon_c(r_s, \zeta). \quad (11)$$

The short-range behavior of  $g_{xc}$  is determined by the  $1/u$  Coulomb repulsion, which gives raise to the cusp condition<sup>17</sup>

$$\frac{dg_{xc}}{du} \Big|_{u=0} = g_{xc} \Big|_{u=0}. \quad (12)$$

The function  $\bar{g}_{xc}$  satisfies a modified cusp condition<sup>2,11</sup> which can be derived from Eqs. (3) and (12). A quite accurate estimate of the  $r_s$  and  $\zeta$  dependence of the short-range expansion coefficients of  $g_{xc}$  and  $\bar{g}_{xc}$  has been recently obtained by solving a scattering problem in a screened Coulomb potential which describes the effective electron-electron interaction in a uniform electron gas – the extended Overhauser model.<sup>11</sup>

The long-range part of the nonoscillatory  $g_{xc}$  corresponds to the small- $k$  behavior of the static structure factor, which is determined by the plasmon contribution, proportional to  $k^2$ , and by the single-pair and multipair quasiparticle-quasihole excitation contributions, proportional to  $k^5$  and  $k^4$  respectively,<sup>18,19</sup>

$$S_{xc}(r_s, \zeta, k \rightarrow 0) = \frac{k^2}{2\omega_p(r_s)} + O(k^4), \quad (13)$$

where  $\omega_p(r_s) = \sqrt{3/r_s^3}$  is the plasma frequency. Equation (13) is called the plasmon sum rule. There is no  $k^3$  term in the small- $k$  expansion of  $S_{xc}$ .<sup>8,20,21</sup> Since, when  $k \rightarrow 0$ , the exchange-only static structure factor  $S_x$  is equal to

$$S_x(\zeta, k \rightarrow 0) = \frac{3}{8} \left[ (1 + \zeta)^{2/3} + (1 - \zeta)^{2/3} \right] \frac{k}{k_F} - \frac{k^3}{16k_F^3}, \quad (14)$$

there must be a linear term and a cubic term in the small- $k$  expansion of the correlation static structure factor  $S_c$  which cancel with the exchange. In real space, these terms correspond to long-range tails  $\propto u^{-4}$  and  $\propto u^{-6}$  respectively.<sup>2,20</sup> The nonoscillatory exchange-correlation pair-distribution function has a long-range tail<sup>8,20</sup>  $\propto u^{-8}$ . The high-density limit of the random-phase approximation (RPA) exactly describes<sup>12</sup> the nonoscillatory long-range part of  $g_{xc}$ , and recovers Eq. (13) through order  $k^2$ .

Armed with these exact constraints, we can discuss the strengths and weaknesses of previous analytic models, which unlike our present model break down<sup>9,10</sup> outside the metallic density range  $1 \lesssim r_s \lesssim 10$ .

The Perdew-Wang model<sup>2</sup> was largely based on first principles, plus limited fitting to Quantum Monte Carlo data. This model introduced the high-density limit of the RPA as the long-range component of  $g_{xc}$ . But that limit was modelled crudely, leading to violation of the particle-conservation sum rule (and thus to failure for  $r_s \lesssim 0.1$ ). The model did not incorporate the plasmon sum rule, and produced an incorrect  $u^{-5}$  nonoscillatory long-range limit for  $g_{xc}$ . The positivity constraint was violated at low densities, a problem evaded by switching over to a different analytic form for  $r_s > 10$ . In this model, the spin resolution of  $g_{xc}$ , even in its revised form,<sup>10</sup> is less reliable than the total  $g_{xc}$ .

The model of Gori-Giorgi, Sacchetti, and Bachelet<sup>8</sup> was based upon extensive fitting to spin-resolved Quantum Monte Carlo data for  $\zeta = 0$ , and did not address nonzero  $\zeta$ . Their model for  $g_{xc}$ , unlike that of Perdew and Wang, was analytically Fourier-transformable to  $S_{xc}$ . It incorporated the particle-conservation and plasmon sum rules, and the correct  $u^{-8}$  long-range limit for  $g_{xc}$ , but did not build in the important high-density limit of the RPA for large  $u$ , leading to failure for  $r_s \ll 0.8$ . Moreover, small- $u$  errors of the Monte Carlo data were transferred into the model.<sup>11</sup>

### III. NONOSCILLATORY EXCHANGE HOLE

We present here our nonoscillatory model for the exchange hole. This new model satisfies exact short-range and long-range conditions up to the same order as our correlation-hole model (Sec. IV) does.

The exact exchange-only pair-distribution function for the uniform gas is

$$g_x(\zeta, k_F u) = 1 + \frac{1}{2} \{ (1 + \zeta)^2 J[(1 + \zeta)^{1/3} k_F u] + (1 - \zeta)^2 J[(1 - \zeta)^{1/3} k_F u] \}, \quad (15)$$

where

$$J(y) = -\frac{9}{2} \left( \frac{\sin y - y \cos y}{y^3} \right)^2. \quad (16)$$

Our nonoscillatory  $\langle J(y) \rangle$  is parametrized as

$$\begin{aligned} \langle J(y) \rangle = & \frac{-9}{4y^4} \left[ 1 - e^{-A_x y^2} \left( 1 + A_x y^2 + \frac{A_x^2 y^4}{2} + \frac{A_x^3 y^6}{3!} \right) \right] \\ & + e^{-D_x y^2} (B_x + C_x y^2 + E_x y^4 + F_x y^6). \end{aligned} \quad (17)$$

Its spherical Fourier transform,

$$\tilde{J}(k) = \int_0^\infty \langle J(y) \rangle y^2 \frac{\sin(ky)}{ky} dy, \quad (18)$$

is also analytic and is reported in Appendix A. The large- $y$  expansion of Eq. (17) is

$$\langle J(y \rightarrow \infty) \rangle = -\frac{9}{4} y^{-4} + O(e^{-y^2}), \quad (19)$$

while the exact nonoscillatory  $J(y)$  also contains a  $y^{-6}$  long-range term. As explained in Sec. II, the exact nonoscillatory correlation hole has long-range terms  $y^{-4}$  and  $y^{-6}$  which exactly cancel with the exchange,<sup>8,20,21</sup> so that the exact nonoscillatory exchange-correlation hole has a long-range tail<sup>8,20</sup>  $\propto u^{-8}$ . However, as detailed in Sec. IV A, our nonoscillatory correlation-hole model is built without a  $u^{-6}$  long-range term, since this choice corresponds to much simpler equations. We have thus also set the  $y^{-6}$  term to zero in our nonoscillatory exchange-hole model, in order to have an exchange-correlation hole with the exact  $u^{-8}$  long-range behavior.

The six parameters  $A_x$  through  $F_x$  are fixed by requiring that (i) the particle-conservation sum rule is fulfilled, (ii) our  $g_x$  gives zero contribution to the plasmon sum rule, (iii) our  $g_x$  recovers the exact exchange energy, (iv) our  $g_x$  is exact at  $u = 0$  in obedience to the Pauli principle, (v) our  $g_x$  has the exact second derivative at  $u = 0$ , and (vi) the information entropy  $\mathcal{S}[-J(y)]$ ,

$$\mathcal{S}[-J(y)] = \int_0^\infty dy 4\pi y^2 J(y) \ln[-J(y)], \quad (20)$$

is maximized, which ensures that  $J(y)$  is as smooth as possible.<sup>22,23</sup> This last feature is important for the development of exchange-correlation energy density functionals which use the exact exchange hole. The parameter values are  $A_x = 0.77$ ,  $B_x = -0.5$ ,  $C_x = -0.08016859$ ,  $D_x = 0.3603372$ ,  $E_x = 0.009289483$ , and  $F_x = -0.0001814552$ .

Our nonoscillatory model  $g_x$  is compared with the exact exchange at  $\zeta = 0$  and  $\zeta = 1$  in the upper panel of Fig. 1. In the first panel of Fig. 3, the exchange hole  $g_x - 1$  is multiplied by  $(u/r_s)^4$  in order to show how our model (solid line) averages out the oscillations of the exact exchange hole (dashed line).

### IV. NONOSCILLATORY CORRELATION HOLE

Following Perdew and Wang,<sup>2</sup> we write the nonoscillatory part of the correlation hole as the sum of a long-

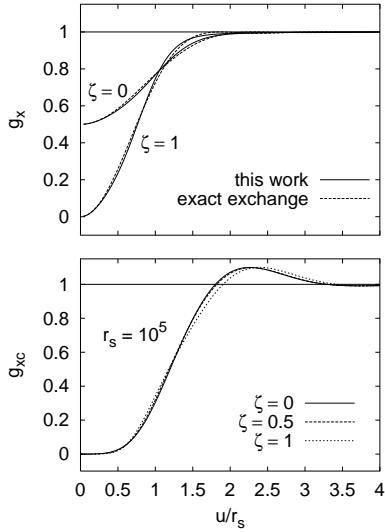


FIG. 1: Upper panel: our nonoscillatory model for exchange in the uniform electron gas is compared with the exact Hartree-Fock curve. Note that  $g_x$  is the  $r_s \rightarrow 0$  limit of  $g_{xc}$ . Lower panel: low-density limit of our analytic model for the exchange-correlation pair-distribution function of the uniform electron gas.

range part and a short-range part,

$$\langle \bar{g}_c(r_s, \zeta, k_F u) \rangle = \left\{ 1 - e^{-d x^2} \left[ 1 + d x^2 + \frac{d^2}{2} x^4 \right] \right\} \times \frac{\phi^3 r_s}{\kappa} \frac{\bar{f}_1(v)}{(k_F u)^2} + e^{-d x^2} \sum_{n=1}^6 c_n x^{n-1}, \quad (21)$$

where  $\kappa = (4/3\pi)(9\pi/4)^{1/3}$ ,  $\phi = [(1+\zeta)^{2/3} + (1-\zeta)^{2/3}]/2$ ,  $x = k_F u/\phi$ , and  $v = \phi \kappa \sqrt{r_s} k_F u$ . The six linear parameters  $c_n$  depend on both  $r_s$  and  $\zeta$ , while the nonlinear parameter  $d$  only depends on  $\zeta$ .

The first term in the r.h.s. of Eq. (21) is the long-range part of our  $\bar{g}_c$ : the function  $\bar{f}_1(v)$  is a new parametrization (see Sec. IV A) of the RPA limit found by Wang and Perdew.<sup>12</sup> We multiplied  $\bar{f}_1(v)/(k_F u)^2$  by a cutoff function which cancels its small- $u$  contributions, so that the long-range part of our  $\bar{g}_c$  vanishes through order  $u^4$  and does not interfere with the short-range part.

For modeling the short-range part, corresponding to the last term in the r.h.s. of Eq. (21), we use our recent results obtained by solving the Overhauser model,<sup>11</sup> which allow us to fix the  $r_s$  and  $\zeta$  dependence of the linear parameters  $c_1$ ,  $c_2$  and  $c_3$  (Sec. IV B). We then use the remaining three linear parameters,  $c_4$ ,  $c_5$  and  $c_6$ , to fulfill the particle-conservation sum rule and the plasmon sum rule, and to recover the “exact” correlation energy (Sec. IV C). Finally, the nonlinear parameter  $d(\zeta)$ , which determines the “mixing” of long-range and short-range contributions, is fixed by imposing the positivity constraint on  $g_{xc}$  when  $r_s \rightarrow \infty$  (Sec. IV D).

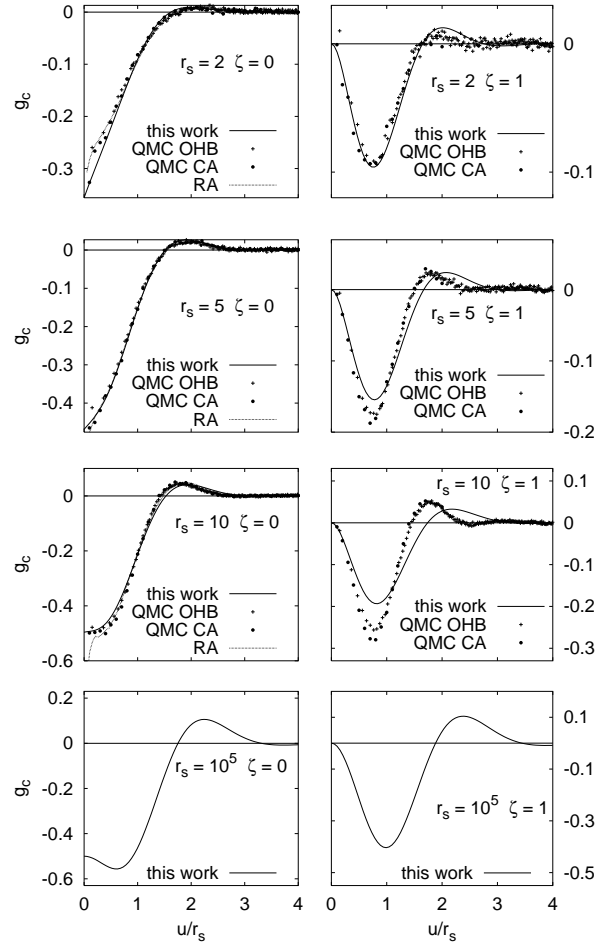


FIG. 2: Pair-correlation function for the uniform electron gas for the paramagnetic ( $\zeta = 0$ ) and ferromagnetic ( $\zeta = 1$ ) state. Our new analytic model is compared with the Diffusion Quantum Monte Carlo results of Ortiz, Harris, and Ballone<sup>14</sup> (OHB), and of Ceperley and Alder<sup>13</sup> (CA). The pair-correlation function corresponding to the local-field-factor model of Richardson and Ashcroft<sup>15</sup> (RA) is also shown. In the two bottom panels, the low-density limit of our  $g_c$  is reported.

### A. Long-range part

As discussed in Refs. 12 and 2, the long-range ( $u \rightarrow \infty$ ) part of the nonoscillatory correlation hole can be obtained from the random-phase approximation by computing its  $r_s \rightarrow 0$  limit. One finds

$$n \langle \bar{g}_c(r_s, \zeta, k_F u) \rangle \rightarrow \phi^3 (\phi k_s)^2 \frac{\bar{f}_1(v)}{4\pi v^2}, \quad (22)$$

where  $k_s$  is the Thomas-Fermi screening wave vector,  $k_s = \kappa \sqrt{r_s} k_F$ . The function  $\bar{f}_1(v)$  is the spherical Fourier transform of the function  $f(z, 0)$  given by Eqs. (29), (34) and (36) of Ref. 12,

$$\bar{f}_1(v) = 2v^2 \int_0^\infty dz z^2 f(z, 0) \frac{\sin(vz)}{vz}, \quad (23)$$

where  $z = k/\phi k_s$  is the proper scaled variable in reciprocal space. The small- and large- $z$  expansion of  $f(z, 0)$  is

$$f(z \rightarrow 0, 0) = -\frac{3}{\pi^2} z + \frac{4\sqrt{3}}{\pi^2} z^2 + O(z^3) \quad (24)$$

$$f(z \rightarrow \infty, 0) = -\frac{2(1-\ln 2)}{\pi^2} z^{-1} + O(z^{-2}). \quad (25)$$

Equation (25) gives the high-density limit of the corresponding correlation energy,

$$\epsilon_c(r_s \rightarrow 0, \zeta) = \frac{(1-\ln 2)}{\pi^2} \phi(\zeta)^3 \ln r_s + O(r_s^0), \quad (26)$$

which is exact at  $\zeta = 0$  and 1, but is slightly different from the exact result for  $0 < \zeta < 1$  (see Refs. 2 and 12 for further details). The small- $z$  expansion of  $f(z, 0)$ , Eq. (24), fulfills the particle-conservation sum rule [ $f(z = 0, 0) = 0$ ], contains a linear term which cancels with the exchange (and corresponds to a long-range tail  $\propto u^{-4}$  in real space, see Sec. II), and fulfills the plasmon sum rule [exact  $z^2$  coefficient, see Eq. (13)].

As said in Secs. II and III, in the small- $z$  expansion of the exact nonoscillatory exchange-correlation hole<sup>8,20,21</sup> there is no  $z^3$  term (which would correspond to a long-range  $u^{-6}$  term). This means that in the correlation hole there must be a  $z^3$  term which cancels with the exchange. However, the exchange  $z^3$  term does not scale as Eq. (22), and so the exact correlation  $z^3$  term cannot be included in  $f(z, 0)$ . Since we want to keep for our  $\bar{g}_c$  the simple form of Eq. (21), but we also want our exchange-correlation hole to have the correct long-range behavior<sup>8,20</sup> ( $\propto u^{-8}$ ), we decided simply to set the  $z^3$  terms (or  $u^{-6}$  terms) equal to 0 both in our exchange- (see Sec. III) and in our correlation-hole models.

We thus parametrize  $\bar{f}_1(v)$  as follows

$$\bar{f}_1(v) = \frac{a_0 + b_2 v + a_1 v^2 + a_2 v^4 + a_3 v^6}{(v^2 + b^2)^4}. \quad (27)$$

With respect to the parametrization given by Perdew and Wang,<sup>2</sup> our Eq. (27) has the advantage that it is analytically Fourier-transformable (see Appendix B), so that the particle-conservation sum rule and the plasmon sum rule can be easily imposed (they are not fulfilled by the Perdew and Wang<sup>2</sup> parametrization). After imposing on our  $\bar{f}_1(v)$  all the exact properties, we are left with one free parameter,  $b$ , which is fixed by a best fit to our RPA data.<sup>12</sup> All the parameter values are reported in Appendix B.

## B. Short-range part

Our  $\bar{g}_c$  has the small- $u$  expansion

$$\langle \bar{g}_c \rangle = c_1 + c_2 \frac{k_F u}{\phi} + (-c_1 d + c_3) \left( \frac{k_F u}{\phi} \right)^2 + O(u^3). \quad (28)$$

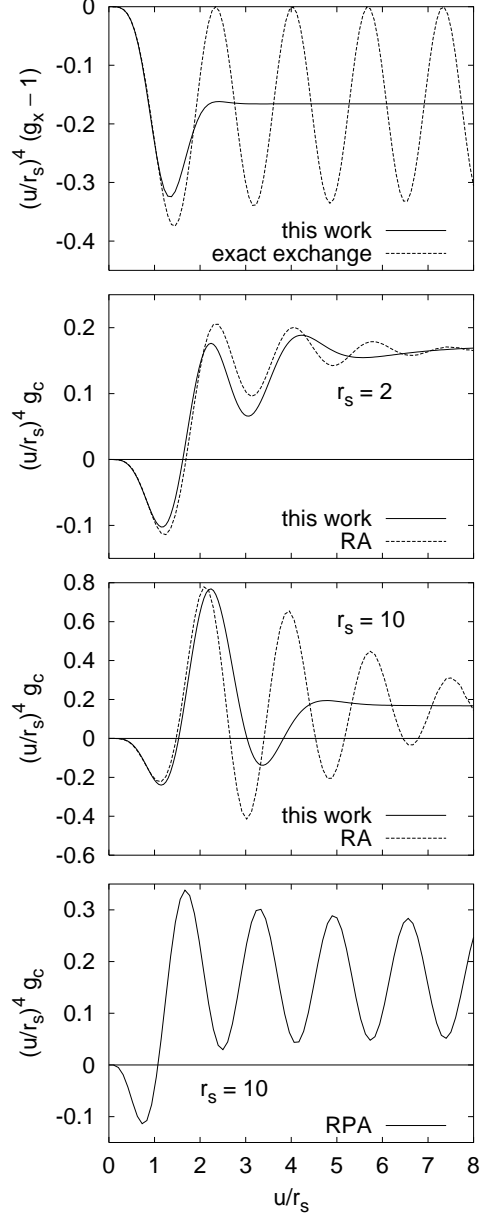


FIG. 3: Upper panel: long-range part of the exchange hole. Our nonsoscillatory model is compared with the exact exchange. Second and third panel: long-range part of the correlation hole. Our nonoscillatory model is compared with  $g_c$  obtained from the Richardson and Ashcroft<sup>15</sup> (RA) local-field factor. In the lowest panel the random-phase-approximation (RPA) result for  $r_s = 10$  is also shown. All curves are for the  $\zeta = 0$  gas.

In order to recover the short-range behavior obtained by solving the Overhauser model,<sup>11</sup> we require

$$c_1 = \frac{(1-\zeta^2)}{2} \left[ \bar{a}_0^{\uparrow\downarrow}(r_s^{\uparrow\downarrow}) - 1 \right] \quad (29)$$

$$c_2 = \phi \left( \frac{4}{9\pi} \right)^{1/3} \frac{(1-\zeta^2)}{2} \left[ \frac{(1+\zeta)^{1/3} + (1-\zeta)^{1/3}}{2} \right] \bar{a}_1^{\uparrow\downarrow}(r_s^{\uparrow\downarrow}) \quad (30)$$

$$c_3 = \phi^2 \left[ \left( \frac{4}{9\pi} \right)^{2/3} \bar{a}_2(r_s, \zeta) - \frac{(1+\zeta)^{8/3} + (1-\zeta)^{8/3}}{20} \right] + c_1 d, \quad (31)$$

where  $r_s^{\uparrow\downarrow} = 2r_s/[(1+\zeta)^{1/3} + (1-\zeta)^{1/3}]$ , and  $\bar{a}_0^{\uparrow\downarrow}$ ,  $\bar{a}_1^{\uparrow\downarrow}$  and  $\bar{a}_2(r_s, \zeta)$  are given by Eqs. (36), (37) and (46) of Ref. 11. In this way, the modified cusp condition is exactly satisfied.<sup>11</sup>

### C. Sum rules

We want our correlation hole to satisfy the particle-conservation sum rule and the plasmon sum rule, and to recover the “exact” correlation energy. Our new parametrization of the function  $\bar{f}_1(v)$  satisfies the particle-conservation sum rule, and recovers the exact plasmon coefficient and the  $\ln r_s$  term of the resulting correlation energy. Thus, we only have to require that the remaining part of our  $\bar{g}_c$  gives zero contribution to (i) the particle-conservation sum rule and (ii) the plasmon sum rule, and (iii) recovers the correlation energy beyond the  $\ln r_s$  term. In this way we have three linear equations for the three parameters  $c_4$ ,  $c_5$  and  $c_6$ :

$$\sum_{n=1}^6 \tilde{c}_n \int_0^\infty e^{-t^2} t^{n+1} dt = AS(\alpha) \quad (32)$$

$$\sum_{n=1}^6 \tilde{c}_n \int_0^\infty e^{-t^2} t^{n+3} dt = AP(\alpha) \quad (33)$$

$$\sum_{n=1}^6 \tilde{c}_n \int_0^\infty e^{-t^2} t^n dt = -AR(\alpha) + E, \quad (34)$$

where  $\tilde{c}_n = c_n/d^{n/2}$ ,  $t = \sqrt{d}k_Fu/\phi$ ,  $A = \phi r_s d/\kappa$ ,  $\alpha = \phi^2 \kappa (r_s/d)^{1/2}$ , and

$$S(\alpha) = \int_0^\infty \bar{f}_1(\alpha t) e^{-t^2} (1 + t^2 + \frac{1}{2}t^4) dt \quad (35)$$

$$P(\alpha) = \int_0^\infty \bar{f}_1(\alpha t) e^{-t^2} t^2 (1 + t^2 + \frac{1}{2}t^4) dt \quad (36)$$

$$R(\alpha) = \int_0^\infty \frac{\bar{f}_1(\alpha t)}{t} \left[ 1 - e^{-t^2} (1 + t^2 + \frac{1}{2}t^4) \right] dt \quad (37)$$

$$E = \frac{2r_s d}{3\phi^2} \left( \frac{9\pi}{4} \right)^{2/3} \epsilon_c(r_s, \zeta). \quad (38)$$

The functions  $S(\alpha)$ ,  $P(\alpha)$  and  $R(\alpha)$  can be obtained analytically and are reported in Appendix C. The param-

eters  $c_4$ ,  $c_5$  and  $c_6$  are then equal to

$$\tilde{c}_4 = \{100\sqrt{\pi}(3\pi - 8)\tilde{c}_1 + (690\pi - 2048)\tilde{c}_2 + \sqrt{\pi}(225\pi - 672)\tilde{c}_3 + (8192 - 2100\pi)AS(\alpha) + AP(\alpha)(600\pi - 2048) + 960\sqrt{\pi}[AR(\alpha) - E]\}/[4(512 - 165\pi)] \quad (39)$$

$$\tilde{c}_5 = 2\{(30\pi - 128)\tilde{c}_1 - 8\sqrt{\pi}\tilde{c}_2 + (39\pi - 128)\tilde{c}_3 - 144\sqrt{\pi}AS(\alpha) + 16\sqrt{\pi}AP(\alpha) - 256[AR(\alpha) - E]\}/(512 - 165\pi) \quad (40)$$

$$\tilde{c}_6 = \{\sqrt{\pi}(180\pi - 624)\tilde{c}_1 + (150\pi - 512)\tilde{c}_2 + \sqrt{\pi}(135\pi - 432)\tilde{c}_3 + (3072 - 1260\pi)AS(\alpha) + AP(\alpha)(360\pi - 1024) - 480\sqrt{\pi}[AR(\alpha) - E]\}/[6(165\pi - 512)]. \quad (41)$$

### D. Positivity constraint in the low-density limit

The nonlinear parameter  $d$  can be fixed by imposing the condition that  $\bar{g}_{xc}$  remains positive when  $r_s \rightarrow \infty$ . The short-range behavior imposed on our  $\bar{g}_c$  ensures that the small- $u$  expansion of the corresponding  $\bar{g}_{xc}$  has coefficients which are always  $\geq 0$  through order  $u^2$ , and which become zero in the low-density or strongly-correlated limit. We have checked that, if we want to have a positive  $\bar{g}_{xc}$  for all densities, we only need to require that also the  $u^3$  coefficient (equal to  $c_4 - d c_2$ ) becomes 0 when  $r_s \rightarrow \infty$ , according to the cusp condition for parallel-spin pairs.<sup>8,11,17</sup> We thus have an equation for  $d(\zeta)$ :

$$\lim_{r_s \rightarrow \infty} c_4(r_s, \zeta) - d(\zeta)c_2(r_s, \zeta) = 0. \quad (42)$$

Equation (42) is rather complicated since  $c_4$  also depends nonlinearly on  $d$ . However, it can be solved numerically for each  $\zeta$ , and, when the Perdew-Wang<sup>24</sup> parametrization of the correlation energy is used in Eq. (38), the result is very well fitted by

$$d(\zeta) = d(0) \left[ (1 + \zeta)^{2/3} + (1 - \zeta)^{2/3} - 1 \right], \quad (43)$$

with  $d(0) = 0.131707$ .

## V. RESULTS FOR THE EXCHANGE-CORRELATION HOLE

In the next three subsections we present and discuss our results for the nonoscillatory  $g_x$ ,  $g_c$  and  $g_{xc}$  in the whole ( $0 < r_s < \infty$ ) density range. We have used the correlation energy  $\epsilon_c$  as parametrized by Perdew and Wang,<sup>24</sup> which was built with the Quantum Monte Carlo data of Ref. 13 as an input. It is however straightforward to build into our equations an *ab initio*  $\epsilon_c$  for the 3D uniform gas when available.<sup>25</sup>

### A. Metallic densities

In the six upper panels of Fig. 2 we compare our analytic  $g_c$  with the Quantum Monte Carlo (QMC) data

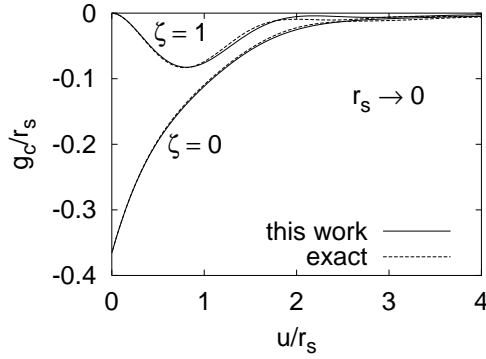


FIG. 4: Pair-correlation function for the uniform electron gas for the paramagnetic ( $\zeta = 0$ ) and ferromagnetic ( $\zeta = 1$ ) state in the high density ( $r_s \rightarrow 0$ ) limit. The result from our analytic model is compared with the exact calculation of Refs. 9,16.

of Ceperley and Alder<sup>13</sup> (CA) and of Ortiz, Harris and Ballone<sup>14</sup> (OHB) for  $r_s = 2, 5$  and  $10$ , and for  $\zeta = 0$  (left) and  $\zeta = 1$  (right). In the  $\zeta = 0$  case, we also report  $g_c$  as obtained by the dynamic local-field-factor model of Richardson and Ashcroft<sup>15</sup> (RA) via the fluctuation-dissipation theorem. The RA model yields very accurate correlation energies  $\epsilon_c(r_s, \zeta = 0)$ ,<sup>26</sup> and we find that the RA  $g_c$  is in very good agreement with QMC data except at small  $u$ . The limit  $u \rightarrow 0$  is not correctly included in the RA parametrization of the local-field factor, which violates the Pauli principle.

We see that our model is in fair agreement with QMC data for the paramagnetic gas. In the ferromagnetic case, where the pair-correlation function shows stronger oscillations even at intermediate densities, the agreement is less satisfactory (as in the model of Ref. 2). This is not surprising, since our model does not take into account the energetically unimportant oscillations: it only includes the minimum number of oscillations needed to fulfill the sum rules. This is evident in the second and third panel of Fig. 3, where  $g_c$  is multiplied by  $(u/r_s)^4$ . In this way, the long-range oscillations are amplified and become clearly visible even at metallic densities: we can thus compare our model (solid line) with the RA result (dashed line). This is done at  $r_s = 2$  and  $10$ . The many exact properties imposed on the RA local-field factor and the first three left panels of Fig. 2 suggest that the long-range part of the RA  $g_c$  is very reliable and that the oscillations are probably accurately described. One clearly sees in Fig. 3 how our model follows the first oscillation and averages out the others. In the lowest panel of Fig. 3, the long-range oscillations of the random-phase approximation (RPA)  $g_c$  at  $r_s = 10$  are also shown. At large  $r_s$ , the RPA oscillations of  $g_c$  tend to cancel the ones of  $g_x$  (first panel), while the effect of a dynamic local-field factor clearly inverts this tendency: the oscillations of the RA  $g_c$  (second and third panel) are almost in phase with the oscillations of  $g_x$ .

## B. High density

In the high-density limit,  $g_c = 2\bar{g}_c$  goes to zero, so that  $g_{xc} \rightarrow g_x$ . It has been shown<sup>2,9,16</sup> that in the  $r_s \rightarrow 0$  limit  $g_c/r_s$  remains finite and goes to a well defined function of  $u/r_s$ , which has been computed exactly.<sup>9,16</sup> In Fig. 4 we compare this exact calculation (dashed line) with our model (solid line), computed at  $r_s = 10^{-5}$ , for  $\zeta = 0$  and  $\zeta = 1$ . We see that (i) our model does not break down as  $r_s \rightarrow 0$ , and (ii) there is fair agreement with the exact result. Previous models<sup>2,8</sup> for  $g_c$  usually break down at  $r_s \sim 0.1$ . Feature (i) is due to the new parametrization of  $\bar{f}_1(v)$  which exactly fulfills the particle-conservation sum rule, while feature (ii) is due to the short-range behavior taken from Ref. 11, which includes the exact high-density limit of the short-range coefficients.

## C. Low density

In the low-density or strongly-correlated limit, we expect that  $g_{xc}$  (equal to  $\bar{g}_{xc}$  in this case) does not depend on  $\zeta$ , since in this limit the Pauli principle becomes irrelevant with respect to the Coulomb repulsion. In the lower panel of Fig. 1 we report our model at  $r_s = 10^5$  for three different values of the spin polarization  $\zeta$ . We see that the  $\zeta$  dependence of our low-density  $g_{xc}$  is indeed very weak, and that, unlike previous parametrizations,<sup>2,8</sup> our model never gives raise to an unphysical negative pair-distribution function. Figure 1 also offers a view on the same scale of the extreme high-density limit of  $g_{xc}$  (equal to the exchange-only pair-distribution function, first panel) and of the extreme low-density limit (second panel). We see how the  $\zeta$  dependence of  $g_{xc}$ , which is very strong in the  $r_s \rightarrow 0$  limit, is cancelled by correlation in the  $r_s \rightarrow \infty$  limit. The low-density limit of our  $g_c = g_{xc} - g_x$  is reported in the two lowest panels of Fig. 2 for  $\zeta = 0$  and  $\zeta = 1$ .

## VI. SPIN RESOLUTION

We can define spin-resolved pair-distribution functions which describe spatial correlations between  $\uparrow\uparrow$ ,  $\downarrow\downarrow$ , and  $\uparrow\downarrow$  electron pairs. Their normalization is such that the spin-averaged  $g_{xc}$  of Eq. (1) is equal to

$$g_{xc} = \left(\frac{1+\zeta}{2}\right)^2 g_{xc}^{\uparrow\uparrow} + \left(\frac{1-\zeta}{2}\right)^2 g_{xc}^{\downarrow\downarrow} + \left(\frac{1-\zeta^2}{2}\right) g_{xc}^{\uparrow\downarrow}. \quad (44)$$

While the spin resolution of the exchange-only pair-distribution function  $g_x$  is well known,<sup>2</sup> the correlation part is much more delicate, and an accurate analytic representation is only available<sup>8</sup> for  $\zeta = 0$  in the density range  $0.8 \leq r_s \leq 10$ .

The model presented in Sec. IV can be used to build up spin-resolved correlation functions provided that the spin

resolution of the input quantities is known. The input quantities are (i) the RPA long-range part, (ii) the short-range coefficients from the solution of the Overhauser model, and (iii) the correlation energy. Once these input quantities are known, in fact, one can build, say,  $\bar{g}_c^{\uparrow\downarrow}$ , starting from the same Eq. (21), using the RPA  $\uparrow\downarrow$  long-range part, and putting the  $\uparrow\downarrow$  short-range coefficients into Eqs. (29)-(31), and  $\epsilon_c^{\uparrow\downarrow}$  into Eqs. (39)-(41). Finally, the positivity constraint of  $g_{xc}^{\uparrow\downarrow}$  in the low-density limit can be applied to find  $d_{\uparrow\downarrow}(\zeta)$ , as done in Sec. IV D.

The first point is thus to see whether the quantities (i)-(iii) are available in their spin-resolved contributions. The RPA long-range part is easily spin-resolved for the  $\zeta = 0$  gas,<sup>8,10</sup> while its spin resolution in the partially polarized gas is less trivial. The short-range coefficients from the Overhauser model are available as  $\uparrow\uparrow$ ,  $\downarrow\downarrow$  and  $\uparrow\downarrow$  separate contributions.<sup>11</sup> The correlation energy represents the major problem: at  $\zeta = 0$  it can be easily spin resolved in the high- and low-density limits, while at intermediate densities the best estimate is probably the one given in Ref. 8. Almost nothing about the spin resolution of  $\epsilon_c$  is known for the  $\zeta \neq 0$  gas, except in the extreme low-density limit, when the system becomes  $\zeta$ -independent.

Here, we show results for  $g_c^{\uparrow\downarrow}$  in three cases: the extreme low-density limit, the high-density limit of the paramagnetic gas, and the  $r_s = 2$ ,  $\zeta = 0$  case. The low-density limit must be treated first, since it is necessary to determine  $d_{\uparrow\downarrow}(\zeta)$  through the positivity constraint on  $g_{xc}^{\uparrow\downarrow}$  when  $r_s \rightarrow \infty$ .

When  $\zeta = 0$ , the spin-resolution within RPA is very simple: up-up and up-down interactions contribute the same amount to correlation.<sup>8,10</sup> The long-range part of our  $\bar{g}_c^{\uparrow\downarrow}$  can thus be built using the function  $\bar{f}_1(v)$  of Eq. (27) with the same parameters of Appendix B. While the spin-averaged nonoscillatory long-range behavior computed within RPA is also exact beyond it at all densities, its spin resolution is exact beyond RPA only when  $r_s \rightarrow 0$ .<sup>27</sup> We keep on using it even in the extreme low-density limit, since it is the only way to build up a spin-resolved  $g_c$  starting from our model. As we shall see, the results obtained are reasonable, and justify our choice. When  $r_s \rightarrow \infty$ , we expect the statistics to be energetically unimportant,<sup>28</sup> so that  $\epsilon_{xc}^{\uparrow\uparrow} = \epsilon_{xc}^{\downarrow\downarrow} = \epsilon_{xc}^{\uparrow\downarrow} = \epsilon_{xc}$ . We thus find  $\epsilon_c^{\uparrow\downarrow} = \epsilon_{xc} = -0.892/r_s$ , where the numerical coefficient corresponds to the Perdew-Wang parametrization<sup>24</sup> of  $\epsilon_c$ . The positivity constraint on  $g_{xc}^{\uparrow\downarrow}$  gives

$$d_{\uparrow\downarrow}(\zeta) = d_{\uparrow\downarrow}(0) \left[ (1 + \zeta)^{2/3} + (1 - \zeta)^{2/3} - 1 \right], \quad (45)$$

with  $d_{\uparrow\downarrow}(0) = 0.0885717$ . The results for  $g_{xc}^{\uparrow\downarrow}$  are shown in Fig. 5, at  $r_s = 10^5$ , for  $\zeta = 0$  and  $\zeta = 1$ .

For the high-density limit of the paramagnetic gas, all the spin-resolved input quantities are exactly known. It is thus the best case to test our model. When  $r_s \rightarrow 0$ , the spin-resolution from RPA is exact also beyond it: the long-range part of  $\bar{g}_c^{\uparrow\downarrow}$  is in this case *exactly* described

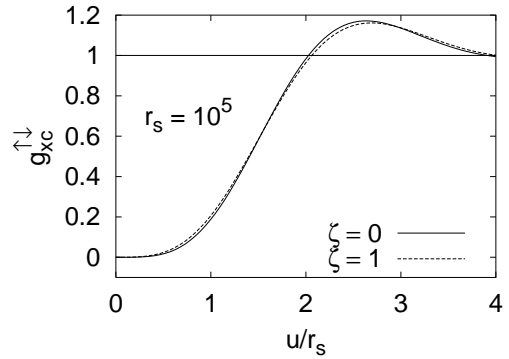


FIG. 5: Up-down pair-distribution function for the uniform electron gas in the low-density limit.

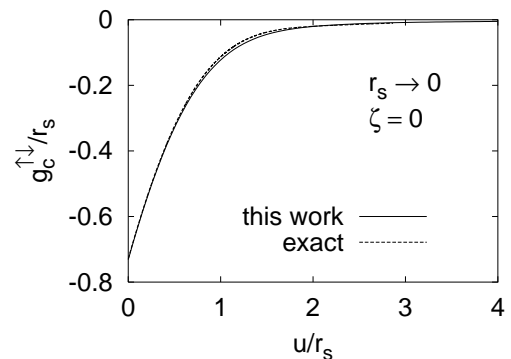


FIG. 6: Up-down pair-correlation function for the paramagnetic ( $\zeta = 0$ ) uniform electron gas in the high density ( $r_s \rightarrow 0$ ) limit. The result from our analytic model is compared with the exact calculation of Ref. 16.

by Eq. (27) with the parameters of Appendix B. The correlation energy, in this limit,<sup>8,20</sup> is simply equal to the spin-averaged correlation energy of Eq. (26) with  $\zeta$  set to zero. The short-range  $\uparrow\downarrow$  coefficients from Ref. 11 include the exact spin-resolved high-density limit of the  $\zeta = 0$  gas. The so-obtained  $g_c^{\uparrow\downarrow}$  is shown in Fig. 6, together with the exact calculation from Ref. 16, which is, in this case, equal to the RPA result. We find very good agreement.

At metallic densities, we used the spin-resolved  $\epsilon_c$  for the  $\zeta = 0$  gas from Ref. 8, and the RPA spin resolution for the long-range part. In Fig. 7, we report our results for  $g_c^{\uparrow\downarrow}$  and  $g_c^{\uparrow\uparrow} = 2g_c - g_c^{\uparrow\downarrow}$  at  $r_s = 2$ , together with the QMC data of Ref. 14, and with the values that we have obtained from the Richardson and Ashcroft (RA) local-field factors.<sup>15</sup> We see that our result is reasonable, but does not accurately agree with the QMC data. In this respect, the RA results are much better for  $u/r_s \gtrsim 0.7$ , while they blow up in the short-range part, since they do not satisfy the Pauli principle. As said, the spin resolution is very delicate, so that an analytic model is very difficult to build up. The best analytic representation of  $g_c^{\uparrow\downarrow}$  and  $g_c^{\uparrow\uparrow}$  at metallic densities is probably the one of Ref. 8, which was built to interpolate the QMC data of

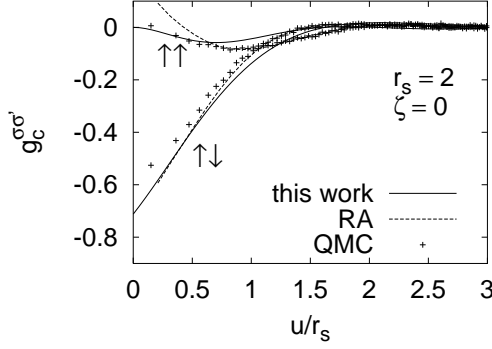


FIG. 7: Spin-resolved pair-correlation functions for the paramagnetic uniform electron gas at density  $r_s = 2$ . The present model is compared with the Quantum Monte Carlo (QMC) data from Ref. 14 and with the result obtained from the local-field factors of Richardson and Ashcroft<sup>15</sup> (RA).

Ref. 14 accurately.

## VII. WAVEVECTOR ANALYSIS OF THE KINETIC ENERGY OF CORRELATION

Wavevector analysis is usually a study of the static structure factor of Eq. (5). The wavevector analyses of the correlation energy and of the potential energy of correlation have often been reported,<sup>8,26,29</sup> while the kinetic energy of correlation  $t_c$  is much less studied. We can decompose  $t_c(r_s, \zeta)$  into contributions from different wavevectors of a density fluctuation,

$$t_c(r_s, \zeta) = \frac{3}{2} \int_0^\infty dq q^2 \mathcal{T}_c(r_s, \zeta, q), \quad (46)$$

where  $q = k/k_F$ , and

$$\mathcal{T}_c(r_s, \zeta, q) = \frac{2k_F}{3\pi} \frac{[\overline{S}_c(r_s, \zeta, q) - S_c(r_s, \zeta, q)]}{q^2}. \quad (47)$$

The small- $q$  limit of  $\mathcal{T}_c$  can be obtained by the plasmon sum rule,

$$\mathcal{T}_c(r_s, \zeta, q \rightarrow 0) = \frac{\sqrt{3}}{4} r_s^{-3/2} + O(q^2), \quad (48)$$

and its leading term is independent of  $\zeta$ , as expected from Eq. (13). To write down the large- $q$  limit of  $\mathcal{T}_c$  we need to expand  $\overline{S}_c$  and  $S_c$  for large arguments. We know that<sup>8,17,20,30</sup>

$$S_c(r_s, \zeta, q \rightarrow \infty) = -\frac{4}{3\pi k_F} \frac{2g_{xc}(r_s, \zeta, u = 0)}{q^4} + O(q^{-6}), \quad (49)$$

from which we can also obtain the large- $q$  limit of  $\overline{S}_c$ ,

$$\overline{S}_c(r_s, \zeta, q \rightarrow \infty) = \frac{\overline{\gamma}}{q^4} + O(q^{-6}), \quad (50)$$

where

$$\overline{\gamma} = -\frac{8}{3\pi} \left( \frac{4}{9\pi} \right)^{1/3} \frac{1}{r_s} \int_0^{r_s} r'_s g_{xc}(r'_s, \zeta, u = 0) dr'_s. \quad (51)$$

Through the cusp condition of Eq. (12), we see that the large- $q$  limit of  $\overline{S}_c$  is determined by the coefficient of  $u/r_s$  in the small- $u$  expansion of  $\overline{g}_c$ ,  $\overline{a}_1(r_s, \zeta)$  [see Eqs. (35) and (37) of Ref. 11], related to  $c_2(r_s, \zeta)$  of Eq. (30) by  $\overline{a}_1 = (9\pi/4)^{1/3} c_2/\phi$ . We thus have

$$\mathcal{T}_c(r_s, \zeta, q \rightarrow \infty) = \frac{8}{9\pi^2} \frac{\left[ 2g_{xc}(r_s, \zeta, u = 0) - 2\frac{\overline{a}_1(r_s, \zeta)}{r_s} \right]}{q^6}. \quad (52)$$

In Fig. 8, we report  $\mathcal{T}_c$  for the  $\zeta = 0$  gas, for two different densities,  $r_s = 2$  and  $r_s = 5$ . We clearly see that the small wavevector contribution to  $t_c$  comes from the kinetic energy of the long-wavelength zero-point plasmons, and that the decay of the plasmon contribution with increasing wavevector  $k$  is gradual. The corresponding result from the Richardson and Ashcroft local field factor<sup>15</sup> is also shown. The Richardson-Ashcroft model gives a good description of plasmon dispersion and damping.<sup>31</sup>

It is also interesting to compare  $\mathcal{T}_c$  with the decomposition of the kinetic energy of correlation into contributions from different wavevectors of a quasi-electron. For  $\zeta = 0$ , we can write

$$t_c(r_s, \zeta = 0) = \frac{3}{2} \int_0^\infty dq q^2 n_c(r_s, \zeta = 0, q) (k_F q)^2. \quad (53)$$

Here  $n_c$  is the correlation contribution to the momentum distribution,  $n_c(q) = n(q) - n_0(q)$ , and  $n_0$  is the Fermi step function. The leading term in the small- $q$  expansion of  $k_F^2 q^2 n_c$  is proportional to  $q^2$ , and is thus rather different from the corresponding behavior of  $\mathcal{T}_c$ , Eq. (48). On the other hand, in the large- $q$  limit we have<sup>30</sup>

$$k_F^2 q^2 n_c(r_s, \zeta = 0, q \rightarrow \infty) = \frac{8}{9\pi^2} \frac{g_{xc}(r_s, \zeta = 0, u = 0)}{q^6}, \quad (54)$$

a behavior very similar to Eq. (52). This is not surprising, since the large- $q$  limits of both  $S_c$  and  $n_c$  are determined by the kinks in the many body wavefunction which occur whenever two electrons are at the same position  $\mathbf{r}$ . In the  $r_s \rightarrow 0$  limit, Eqs. (52) and (54) become equal. A study of the equations linking  $S_c$  and  $n_c$  from the point of view of density matrix functional theory is reported in Ref. 32.

## VIII. CONCLUSIONS AND FUTURE DIRECTIONS

The known exact constraints summarized in Sec. II, plus the random phase approximation for long-range ( $u \rightarrow \infty$ ) correlation, the extended Overhauser model<sup>11</sup>

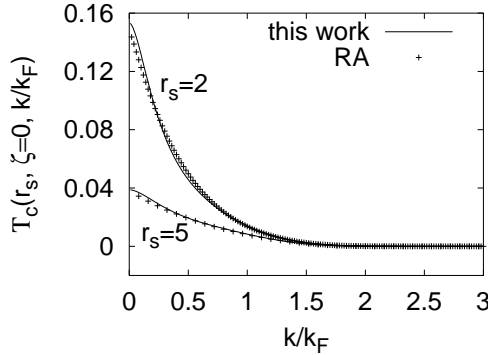


FIG. 8: Wavevector analysis of the kinetic energy of correlation at  $r_s = 2$  and  $r_s = 5$  for the paramagnetic gas. The function  $T_c(r_s, \zeta, k)$  is defined in Eq. (47). The present work is compared with the result obtained from the Richardson and Ashcroft<sup>15</sup> (RA) local-field factor.

for short-range ( $u \rightarrow 0$ ) correlation, and the correlation energy  $\epsilon_c(r_s, \zeta)$ , suffice to determine the pair distribution function  $g_{xc}(r_s, \zeta, k_F u)$  of a uniform electron gas over the whole density range, including the high-density ( $r_s \rightarrow 0$ ) and low-density ( $r_s \rightarrow \infty$ ) limits, apart from energetically-unimportant long-range oscillations. The analytic formulas we have so constructed for the coupling-constant-averaged  $\bar{g}_{xc}$  should be useful for further developments and applications of density-functional approximations for the exchange-correlation energy of a non-uniform density.

For metallic densities ( $2 < r_s < 10$ ) with  $\zeta = 0$  or 1, our  $g_{xc}$  is in good agreement with Quantum Monte Carlo.<sup>13,14</sup> In the same density range for  $\zeta = 0$ , it also agrees with the  $g_{xc}$  we have calculated from the Richardson-Ashcroft<sup>15</sup> dynamic local-field factor, except near  $u = 0$  where the Richardson-Ashcroft model was found to break down (although this model seems to describe the long-range oscillations correctly). In the  $r_s \rightarrow 0$  limit for small  $k_F u$ , our  $g_{xc}$  agrees with the results of perturbation theory to zero-th (exchange) or first order<sup>9,16</sup> in the electron-electron interaction. The static structure factor  $S_{xc}$  is also modelled accurately, neglecting the non-analytic structure of the exact  $S_{xc}$  at  $k = 2k_F$  arising from long-range oscillations.<sup>32</sup>

Our formulas can also be used to spin-resolve  $g_{xc}$  into  $\uparrow\uparrow$ ,  $\downarrow\downarrow$ , and  $\uparrow\downarrow$  components (Sec. VI), when the spin resolution of  $\epsilon_c$  is known (as it is in the high- and low-density limits).

We have also examined two physically-different wavevector analyses of the kinetic energy of correlation in the uniform electron gas, finding them the same only in the limits of large wavevector and high density. We have also found that the decay of the plasmon contribution with increasing wavevector  $k$  is gradual.

In the future, it may be possible to construct the correlation energy  $\epsilon_c(r_s, \zeta)$  and its spin resolution  $\epsilon_c^{\sigma\sigma'}(r_s, \zeta)$  directly by interpolation between known limits,<sup>25</sup> with-

out using *any* Monte Carlo or other data. The extended Overhauser model<sup>11</sup> might be evaluated for  $\zeta$  different from zero, to test and refine the spin-scaling relations used in Ref. 11. The extended Overhauser model can also be made more selfconsistent.<sup>33</sup>

A small FORTRAN subroutine which numerically evaluates our  $\bar{g}_c$  [Eq. (21)] can be obtained upon request to gp.giorgi@caspur.it.

## Acknowledgments

This work was supported by the Fondazione Angelo Della Riccia (Firenze, Italy), the MURST (the Italian Ministry for University, Research and Technology) through COFIN99, and by the U.S. National Science Foundation under grants DMR-9810620 and DMR-0135678.

## APPENDIX A: NONOSCILLATORY EXCHANGE HOLE IN RECIPROCAL SPACE

In reciprocal space, the exchange-only static structure factor is equal to

$$S_x(\zeta, k/k_F) = 1 + \frac{2}{3\pi} \left[ (1 + \zeta) \tilde{J} \left( \frac{k}{k_F(1 + \zeta)^{1/3}} \right) + (1 - \zeta) \tilde{J} \left( \frac{k}{k_F(1 - \zeta)^{1/3}} \right) \right], \quad (A1)$$

where  $\tilde{J}(k)$  is defined by Eq. (18). From our parametrization of  $\langle J(y) \rangle$  [Eq. (17)] we obtain

$$\begin{aligned} \tilde{J}(k) = & \frac{9\pi}{16} k \left[ 1 - \text{erf} \left( \frac{k}{2\sqrt{A_x}} \right) \right] - \frac{3\sqrt{\pi}}{32} e^{-\frac{k^2}{4A_x}} \times \\ & \left( 9\sqrt{A_x} + \frac{k^2 - 6A_x}{4\sqrt{A_x}} \right) + \frac{\sqrt{\pi}}{4} e^{-\frac{k^2}{4D_x}} \left[ \frac{B_x}{D_x^{3/2}} + \frac{C_x(6D_x - k^2)}{4D_x^{7/2}} + \frac{E_x(60D_x^2 - 20D_xk^2 + k^4)}{16D_x^{11/2}} + \frac{F_x(840D_x^3 - 420D_x^2k^2 + 42D_xk^4 - k^6)}{64D_x^{15/2}} \right]. \quad (A2) \end{aligned}$$

## APPENDIX B: LONG-RANGE CORRELATION HOLE IN RECIPROCAL SPACE

The function  $f(z, 0)$  corresponding to our Eq. (27) is

$$f(z, 0) = \frac{1}{2zb^8} \left\{ a_0 - \frac{e^{-bz}}{48} [48a_0 + (33a_0b - 3a_1b^3 - 3a_2b^5 - 15a_3b^7)z + (9a_0b^2 - 3a_1b^4 - 3a_2b^6 + 9a_3b^8)z^2 + (a_0b^3 - a_1b^5 + a_2b^7 - a_3b^9)z^3] \right\} - \frac{b_2}{6\pi z} \frac{\partial^3 \mathcal{I}(b, z)}{\partial(b^2)^3}, \quad (B1)$$

where

$$\mathcal{I}(b, z) = \frac{1}{2b} [e^{bz} E_1(bz) - e^{-bz} E_1(-bz)], \quad (\text{B2})$$

and, with  $x > 0$ ,

$$E_1(x) = \int_x^\infty \frac{e^{-t}}{t} dt$$

$$E_1(-x) = -\text{Ei}(x) = -\text{PV} \left( \int_{-\infty}^x \frac{e^t}{t} dt \right).$$

Here PV means the Cauchy principal value integral.<sup>34</sup>

The parameter values which satisfy Eqs. (24) and (25), give raise to a zero coefficient for the  $z^3$  term in the small- $z$  expansion of  $f(z, 0)$ , and accurately fit our RPA data,<sup>12</sup> are

$$\begin{aligned} a_0 &= 2b^8 C_0 \\ a_1 &= \frac{6b^3}{\pi^2} [\pi^2 C_0 b^3 + 78b - 256\sqrt{3}] \\ a_2 &= 48b^2/\pi^2 \\ a_3 &= 12/\pi^2 \\ b_2 &= \frac{3b^4}{\pi} [96\sqrt{3} - 36b - b^3 C_0 \pi^2] \\ C_0 &= -2(1 - \ln 2)/\pi^2 \\ b &= 7.8. \end{aligned}$$

### APPENDIX C: ANALYTIC EXPRESSIONS FOR THE FUNCTIONS $S(\alpha)$ , $P(\alpha)$ AND $R(\alpha)$

The three functions of Eqs. (35), (36) and (37), which enter our model for  $\bar{g}_c$ , are given by a linear combination of integrals of the kind

$$\mathcal{I}_m^n(\alpha) = \int_0^\infty \frac{x^n e^{-x^2}}{[(\alpha x)^2 + b^2]^m} dx \quad (\text{C1})$$

$$\mathcal{I}_m^{-1}(\alpha) = \int_0^\infty \frac{1 - e^{-x^2}}{x[(\alpha x)^2 + b^2]^m} dx. \quad (\text{C2})$$

We obtain for  $S(\alpha)$ ,  $P(\alpha)$  and  $R(\alpha)$ :

$$\begin{aligned} S(\alpha) &= a_0 \mathcal{I}_4^0(\alpha) + (a_0 + a_1 \alpha^2) \mathcal{I}_4^2(\alpha) + (\frac{1}{2} a_0 + a_1 \alpha^2 + a_2 \alpha^4) \mathcal{I}_4^4(\alpha) + (\frac{1}{2} a_1 \alpha^2 + a_2 \alpha^4 + a_3 \alpha^6) \mathcal{I}_4^6(\alpha) + (\frac{1}{2} a_2 \alpha^4 + a_3 \alpha^6) \mathcal{I}_4^8(\alpha) + \frac{1}{2} a_3 \alpha^6 \mathcal{I}_4^{10}(\alpha) + b_2 \alpha \times [\mathcal{I}_4^1(\alpha) + \mathcal{I}_4^3(\alpha) + \frac{1}{2} \mathcal{I}_4^5(\alpha)] \end{aligned} \quad (\text{C3})$$

$$\begin{aligned} P(\alpha) &= a_0 \mathcal{I}_4^2(\alpha) + (a_0 + a_1 \alpha^2) \mathcal{I}_4^4(\alpha) + (\frac{1}{2} a_0 + a_1 \alpha^2 + a_2 \alpha^4) \mathcal{I}_4^6(\alpha) + (\frac{1}{2} a_1 \alpha^2 + a_2 \alpha^4 + a_3 \alpha^6) \mathcal{I}_4^8(\alpha) + (\frac{1}{2} a_2 \alpha^4 + a_3 \alpha^6) \mathcal{I}_4^{10}(\alpha) + \frac{1}{2} a_3 \alpha^6 \mathcal{I}_4^{12}(\alpha) + b_2 \alpha \times [\mathcal{I}_4^3(\alpha) + \mathcal{I}_4^5(\alpha) + \frac{1}{2} \mathcal{I}_4^7(\alpha)] \end{aligned} \quad (\text{C4})$$

$$\begin{aligned} R(\alpha) &= a_0 \mathcal{I}_4^{-1}(\alpha) - (a_0 + a_1 \alpha^2) \mathcal{I}_4^1(\alpha) - (\frac{1}{2} a_0 + a_1 \alpha^2 + a_2 \alpha^4) \mathcal{I}_4^3(\alpha) - (\frac{1}{2} a_1 \alpha^2 + a_2 \alpha^4 + a_3 \alpha^6) \mathcal{I}_4^5(\alpha) - (\frac{1}{2} a_2 \alpha^4 + a_3 \alpha^6) \mathcal{I}_4^7(\alpha) - \frac{1}{2} a_3 \alpha^6 \mathcal{I}_4^9(\alpha) - b_2 \alpha \times [\mathcal{I}_4^0(\alpha) + \mathcal{I}_4^2(\alpha) + \frac{1}{2} \mathcal{I}_4^4(\alpha)] + \frac{2a_1 + a_2 b^2 + 2a_3 b^4}{12b^6} + b_2 \frac{5\pi}{32b^7}, \end{aligned} \quad (\text{C5})$$

where  $a_0$ ,  $a_1$ ,  $a_2$ ,  $a_3$ ,  $b_2$  and  $b$  are given in Appendix B. The integrals of the kind (C1) can be written as

$$\mathcal{I}_m^n(\alpha) = \tilde{\mathcal{I}}_m^n(\alpha/b)/b^{2n}, \quad (\text{C6})$$

$$\tilde{\mathcal{I}}_m^n(r) = \int_0^\infty \frac{x^n e^{-x^2}}{[(rx)^2 + 1]^m} dx, \quad (\text{C7})$$

and starting from

$$\tilde{\mathcal{I}}_1^0(r) = \frac{\pi}{2r^2} e^{1/r^2} \left[ 1 - \text{erf} \left( \frac{1}{r} \right) \right] \quad (\text{C8})$$

$$\tilde{\mathcal{I}}_1^1(r) = \frac{1}{2r^2} e^{1/r^2} E_1 \left( \frac{1}{r^2} \right), \quad (\text{C9})$$

can be computed by differentiation with respect to  $\alpha$  and  $b$ . The integrals of the kind (C2) can be also obtained by differentiation with respect to  $b$  of

$$\mathcal{I}_1^{-1}(\alpha) = \frac{e^{b^2/\alpha^2} E_1(b^2/\alpha^2) + \ln(b^2/\alpha^2) + \gamma}{2b^2}, \quad (\text{C10})$$

where  $\gamma = 0.5772156649$ .

---

<sup>1</sup> see, e.g., R.O. Jones and O. Gunnarsson, Rev. Mod. Phys. **61**, 689 (1989).

<sup>2</sup> J. P. Perdew and Y. Wang, Phys. Rev. B **46**, 12947 (1992); erratum **56**, 7018 (1997).

<sup>3</sup> J. P. Perdew, *Electronic Structure of Solids '91*, edited by P. Ziesche and H. Eschrig (Akademie Verlag, Berlin 1991); J. P. Perdew, K. Burke, and M. Ernzerhof, Phys. Rev. Lett. **77**, 3865 (1996); erratum **78**, 1396 (1997).

<sup>4</sup> O. Gunnarsson, M. Jonson, and B. I. Lundqvist, Phys. Lett. A **59**, 177 (1976); Phys. Rev. B **20**, 3136 (1979).

<sup>5</sup> E. Chacón and P. Tarazona, Phys. Rev. B **37**, 4013 (1988).

<sup>6</sup> P. Ziesche, *Electron Correlations and Material Properties 2*, edited by A. Gonis, N. Kioussis and M. Ciftan (Kluwer Academic/Plenum Publishers, New York 2002), and references therein.

<sup>7</sup> J. P. Perdew, K. Burke, and Y. Wang, Phys. Rev. B **54**, 16533 (1996).

<sup>8</sup> P. Gori-Giorgi, F. Sacchetti, and G.B. Bachelet, Phys. Rev. B **61**, 7353 (2000).

<sup>9</sup> V. A. Rassolov, J. A. Pople, and M. A. Ratner, Phys. Rev. B **59**, 15625 (1999).

<sup>10</sup> K. Schmidt, S. Kurth, J. Tao, and J. P. Perdew, Phys. Rev. B **62**, 2227 (2000).

<sup>11</sup> P. Gori-Giorgi and J. P. Perdew, Phys. Rev. B **64**, 155102 (2001).

<sup>12</sup> Y. Wang and J. P. Perdew, Phys. Rev. B **44**, 13298 (1991).

<sup>13</sup> D. M. Ceperley and B. J. Alder, Phys. Rev. Lett. **45**, 566 (1980).

<sup>14</sup> G. Ortiz, M. Harris, and P. Ballone, Phys. Rev. Lett. **82**, 5317 (1999).

<sup>15</sup> C.F. Richardson and N.W. Ashcroft, Phys. Rev. B **50**, 8170 (1994).

<sup>16</sup> V. A. Rassolov, J. A. Pople, and M. A. Ratner, Phys. Rev. B **62**, 2232 (2000).

<sup>17</sup> A. K. Rajagopal, J. C. Kimball, and M. Banerjee, Phys. Rev. B **18**, 2339 (1978).

<sup>18</sup> P. Nozières and D. Pines, Phys. Rev. **111**, 442 (1958).

<sup>19</sup> D. Pines and P. Nozières, *Theory of Quantum Liquids* (Benjamin, New York, 1966).

<sup>20</sup> P. Gori-Giorgi, F. Sacchetti, and G.B. Bachelet, Physica A **280**, 199 (2000).

<sup>21</sup> N. Iwamoto, Phys. Rev. A **33**, 1940 (1986).

<sup>22</sup> M. Ernzerhof and J.P. Perdew, J. Chem. Phys. **109**, 3315 (1998).

<sup>23</sup> J. Antolin, A. Zarzo, and J.C. Angulo, Phys. Rev. A **50**, 240 (1994).

<sup>24</sup> J.P. Perdew and Y. Wang, Phys. Rev. B **45**, 13244 (1992).

<sup>25</sup> M. Seidl and J.P. Perdew, in preparation.

<sup>26</sup> M. Lein, E. K. U. Gross, and J. P. Perdew, Phys. Rev. B **61**, 13431 (2000).

<sup>27</sup> In Refs. 8,10,20 the RPA spin-resolution is assumed exact for the long-range part of  $g_{xc}$  at all densities. Further studies by one of us (P.G.-G.) showed that this is true only when  $r_s \rightarrow 0$ , but with small deviations as  $r_s$  increases, so that the assumption made is still quite accurate at  $r_s \sim 10$ .

<sup>28</sup> This assumption is reasonable, but could be inexact. In the low-density limit, the electron gas becomes  $\zeta$ -independent, since the statistics is irrelevant with respect to Coulomb repulsion, but magnetic order can be present, so that  $g_{xc}^{\uparrow\downarrow}$  may differ from  $g_{xc}^{\uparrow\uparrow}$  for  $u/r_s \gtrsim 1$ . A close comparison of our Figs. 1 and 5 for  $r_s = 10^5$  and  $\zeta = 0$  seems to show this effect. (For  $u/r_s \lesssim 1$  both  $g_{xc}^{\uparrow\downarrow}$  and  $g_{xc}^{\uparrow\uparrow}$  tend to zero in the strongly correlated limit.)

<sup>29</sup> J. Tao, P. Gori-Giorgi, J.P. Perdew, and R. McWeeny, Phys. Rev. A **63**, 32513 (2001).

<sup>30</sup> J. C. Kimball, Phys. Rev. A **7**, 1648 (1973).

<sup>31</sup> K. Tatarczyk, A. Schindlmayr, and M. Scheffler, Phys. Rev. B **63**, 235106 (2001).

<sup>32</sup> P. Gori-Giorgi and P. Ziesche, cond-mat/0205342, submitted to J. Phys.: Condens. Matter.

<sup>33</sup> B. Davoudi, M. Polini, R. Asgari, and M.P. Tosi, cond-mat/0201423, to appear in Phys. Rev. B.

<sup>34</sup> M. Abramowitz and I. Stegun, *Handbook of Mathematical Functions* (Dover Publications Inc., New York, 1965).